



# Within the Protection of COVID-19 Spreading: A Face Mask Detection Model Based on the Neutrosophic RGB with Deep Transfer Learning.

Nour Eldeen Khalifa <sup>1\*</sup>, Mohamed Loey <sup>2</sup>, Ripon K. Chakraborty <sup>3</sup> and Mohamed Hamed N. Taha <sup>1</sup>

<sup>1</sup> Department of Information Technology, Faculty of Computers & Artificial Intelligence, Cairo University, Cairo 12613, Egypt; email: nourmahmoud@cu.edu.eg

<sup>2</sup> Department of Computer Science, Faculty of Computers and Artificial Intelligence, Benha University, Benha 13511, Egypt; email: mloey@fci.bu.edu.eg

<sup>3</sup> School of Engineering & IT, UNSW Canberra at ADFA, Australia; email: r.chakraborty@adfa.edu.au

\*Correspondence Author: nourmahmoud@cu.edu.eg

**Abstract:** COVID-19's fast spread in 2020 compelled the World Health Organization (WHO) to declare COVID-19 a worldwide pandemic. According to the WHO, one of the preventative countermeasures against this type of virus is to use face masks in public places. This paper proposes a face mask detection model by extracting features based on the neutrosophic RGB with deep transfer learning. The suggested model is divided into three steps, the first step is the conversion to the neutrosophic RGB domain. This work is considered one of the first trails of applying neutrosophic RGB conversion to image domain, as it was commonly used in the conversion of grayscale images. The second step is the feature extraction using Alexnet, which has been small number of layers. The detection model is created in the third step using two traditional machine learning algorithms: decision trees classifier and Support Vector Machine (SVM). The Simulated Masked Face dataset (SMF) and the Real-World Mask Face dataset (RMF) are merged to a single dataset with two categories (a face with a mask, and a face without a mask). According to the experimental results, the SVM classifier with the True (T) neutrosophic domain achieved the highest testing accuracy with 98.37%.

**Keywords:** Neutrosophic RGB; COVID-19; Classical Machine Learning; Deep Learning; Face Mask Detection

## 1. Introduction

As COVID spread swiftly throughout the globe in 2020, the World Health Organization was forced to proclaim a worldwide pandemic. In more than 180 nations, more than seven million cases have been diagnosed with COVID-19 with a death rate of 3 percent, according to [1]. Extensive initiatives are underway around the globe to create innovative therapies and vaccinations for the disease. The new coronavirus known as severe acute respiratory syndrome coronavirus 2 (SARS-CoV-2) is a member of the pathogen family that caused respiratory illnesses during the 2002–2003 pandemic (SARS-CoV-1) [2].

COVID-19 is distinguished by a pre-symptomatic phase of transmission, as freshly infected persons may harm others inadvertently. The infection travels by direct touch and across polluted and overcrowded environments. The face mask is an effective way to prevent the COVID-19 spread of airborne particles [3]. According to [4], [5], having to wear face masks in crowded areas and public will help to reduce disease transmission all the time. In many societies, governments face tremendous obstacles and hazards in protecting people from coronavirus. When it comes to the dissemination

and transmission of COVID-19, policymakers confront a slew of concerns and dangers [6]. In several countries, people are required by law to wear face masks in public [7]. These recommendations and rules were created as part of an attempt to combat the rapidly growing number of fatalities in several nations. However, managing a large group of people is getting increasingly difficult. One possible and realistic solution is to have a screening process that includes the identification of someone who does not wear a face mask. Despite a few screening processes, the search for a better approach is still an open research question, particularly in this COVID era.

Artificial intelligence contributes to the fight against the pandemic of COVID-19 in many ways. These days, several AI-powered initiatives focused on data analysis, 'machine learning' or 'big data' are being utilized in a broad variety of fields to anticipate, clarify and control the different health disaster scenarios [8]. AI technology and resources play a crucial role in every aspect of the COVID-19 crisis response, helping to prevent or slow down the spread of the virus through surveillance and contact tracking [9]. Due to significant developments in the domain of machine learning algorithms, face mask recognition technology looks to be effectively handled [10]. This type of technology is more relevant nowadays than it was previously because it's used for static picture recognition and on-monitoring as well as real-time inspection and supervision [11].

Numerous researches have been conducted on various issues relating to COVID-19 and have been solved by the computer science field, for example, tracking COVID-19 geographical infections using real-time tweets [12], investigating the role of developing technology in the fight against the COVID -19 pandemic [13], determining the COVID-19's influence on the electrical industry [14], Using machine learning and deep learning models to classify potential coronavirus treatments on a single human cell [15] and more. Numerous researches focus on the classification and categorization of COVID-19 CT and X-ray images [16]–[19].

Smarandache [20] proposed the principle of Neutrosophic logic in 1995 and then expanded it in 1999 [21]. Neutrosophic logic has been utilized in various disciplines of computer science since that time, including pattern recognition [22], image processing and segmentation [23], and more. This leads to the resolution of many scientific and practical real-life problems in a variety of areas, such as economics [24], [25], agriculture, and space satellite [26]. Neutrosophic [27] is the foundation of a wide family of current mathematical theories that describe both classical and fuzzy analogues. The term neutro-sophy refers to the feeling of neutral thinking, and it is this justification that distinguishes fuzzy and intuitive fuzzy logic from set theory. A neutrosophic set [28] can be a generic method for analyzing data set uncertainty and, in particular, images in the field of artificial intelligence and deep learning. Various works used Neutrosophic theory and set with medical image analysis as presented in [29].

Because people in some countries are compelled by law to wear face masks in public, masked face recognition is a must for dealing with apps such as object detection. To battle and ultimately win the war against the COVID-19 pandemic, policymakers require advice and surveillance of individuals in public areas, particularly crowds, to guarantee that the legislation requiring the use of face masks is implemented. This might be expanded by combining surveillance technology with Artificial Intelligence models.

The remainder of the paper is organized as follows. Section 2 is a synopsis of prior relevant works. Section 3 describes the data set's features. Section 4 describes the suggested model in detail. Section 5 summarizes and analyses the experimental data, and Section 6 offers the conclusions and future work options.

## 2. Related Works

In [30], the authors developed a novel method for identifying the face of the human characterized by the use of a mask or not. While wearing the face mask, they were able to distinguish three different sorts of conditions. Correct facemask wearing, improper facemask wearing, and no facemask wearing. The suggested technique achieved a face detection process accuracy of 98.70%. In [31], Convolutional

neural networks were utilized to suggest a unique approach known as face emotion recognition (FERC). A two-part convolutional neural network served as the foundation for the FERC. The FERC was able to properly depict the emotion with 96% accuracy. Nizam et al. [32] proposed a GAN-based structure capable of automatically eliminating masks enclosing the facial region and reconstructing the image by filling in the missing area. The introduced method produced a full, natural, and realistic picture of the face. Khan et al [9] developed a framework for automatically separating a face image into face parts and subsequently classifying the gender. The scientists used hand-labeled facial pictures to train a segmentation design based on Conditional Random Fields (CRFs). The CRF-based model was utilised to segment a facial picture into six separate classes: mouth, hair, eyes, nose, skin, and back. The proposed framework was almost 93 percent accurate. In [33], the authors used the YOLOv3 with Darknet-53 algorithm for facial detection. The introduced approach was trained on two public datasets including more than 600k images and testing was on the Face Detection Data Set and Benchmark (FDDB) dataset [34]. The introduced approach had reached an accuracy of 93.9%. Canping et al [35] suggested an unique deep neural network (DNN) training framework to speed the training process of the triplet loss-based DNN while improving face recognition performance. The suggested model obtained 97.3 percent accuracy on the LFW benchmark, according to experimental findings [36]. Most of the related work focuses on facial construction and recognition of faces, there are few research focuses if the human wear a mask or not on his/her face. The goal of this study is to identify persons who do not wear medical face masks in order to reduce COVID-19 transmission and spread.

### 3. Datasets Characteristics

To train and test the proposed approach two publicly available masked face dataset are being utilized. The first dataset is Real-World Mask Face (RMF) dataset [37]. The RMF dataset contains 95000 faces, both masked and unmasked. Figure 1 shows samples of peoples wearing masks and without masks. Only 5000 photos were chosen at random for this study's trials in order to balance the number of images for each class, as well as the second dataset.



Figure 1. RMF samples pictures

The Simulated Masked Face (SMF) [38] dataset is the second masked face dataset. The SMF dataset contains 1570 pictures, 785 of which are masked and unmasked faces. Figure 2 depicts several instances of SMF images. The combined dataset contains 3285 pictures for each class, for a total of 6570 images. Each class has 2500 RMF pictures and 785 SMF images.



Figure 2. SMF samples pictures

#### 4. The Proposed Model Structure

The suggested model structure is divided into three parts. The first part involves converting the original RGB domain to neutrosophic domain. The second part involves extracting features from dataset pictures using the Alexnet (A. Krizhevsky et al., 2017) . The third part is the classification process, which employs traditional machine techniques such as decision trees and support vector machines. Figure 3 depicts the suggested model structure in a graphical form. The next three subsections go into the specifics of these parts.

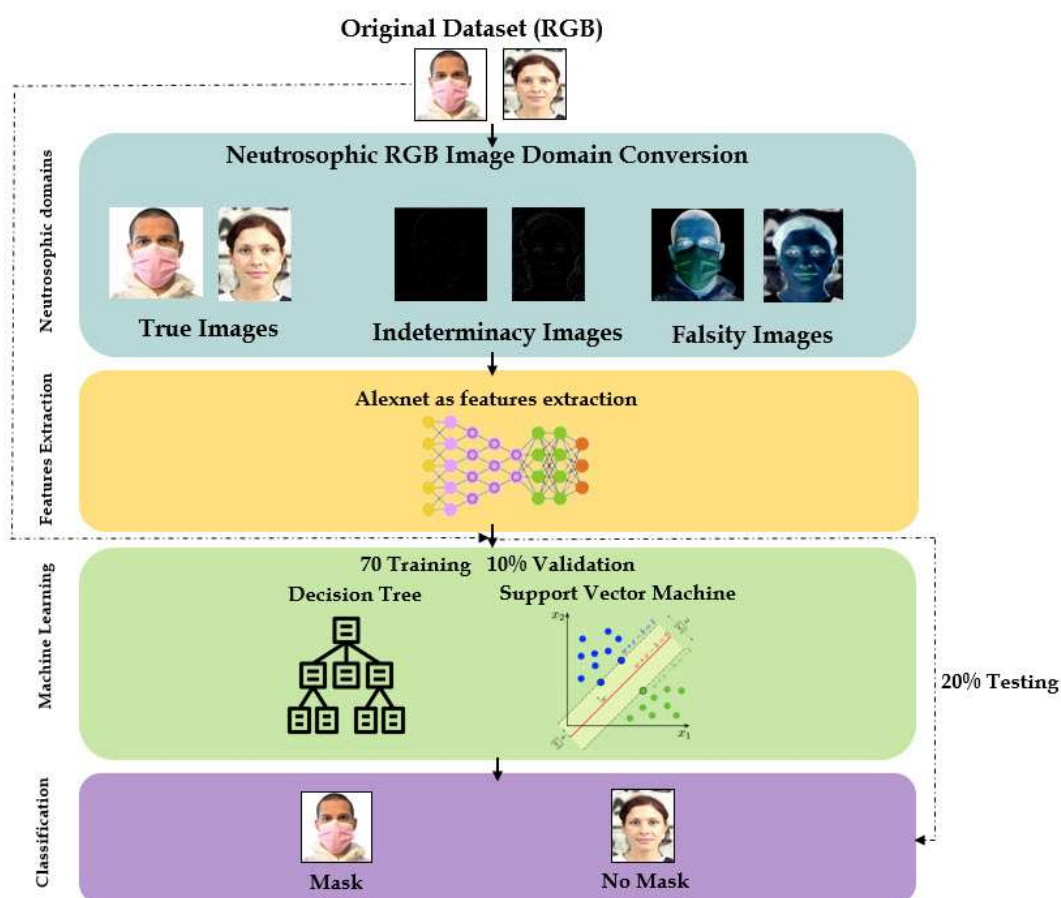


Figure 3. The proposed model structure

### 4.1. Neutrosophic RGB Conversion

The neutrosophic logic (NL) was created and implemented by Florentin Smarandache [39],[40]. In the NL, three neutrosophic subsets, true (T) value, indeterminacy (I) value and falsity (F) value are defined for any event. These neutrosophic values (T, I, F) are commonly used to transform a grayscale image into the neutrosophic image. The introduced research created a new neutrosophic definition on the masked face images, where T exemplify the masked face zone, I exemplify the masked face boundary, and F exemplify the background of image. The image converts to the neutrosophic image (NI) as illustrated in equations 1-4 [25] [41]:

$$NI(a, b) = \{T_{a,b}, I_{a,b}, F_{a,b}\} \tag{1}$$

$$T_{a,b} = \frac{v(a,b) - v_{min}}{v_{max} - v_{min}} \tag{2}$$

$$F_{a,b} = 1 - T_{a,b} \tag{3}$$

$$I_{a,b} = 1 - \frac{U(a,b) - U_{min}}{U_{max} - U_{min}} \tag{4}$$

Let  $v(a, b)$  is the local mean value of related pixels.  $v_{max}$  and  $v_{min}$  are the maximum and minimum absolute difference pixels of the histogram.  $U(a, b)$  is the homogeneity value of  $T(a, b)$ . While  $U_{max}$  and  $U_{min}$  are the maximum and minimum peaks respectively, measured from  $U(a, b)$ .

As mentioned above, the neutrosophic logics are commonly used with the grayscale domain. In this work, the authors introduced the neutrosophic RGB conversion. The main idea is to split the RGB domain into three domains (Red, Green, and Blue). After that, apply the equations of neutrosophic conversion in every domain separately. Then combine the resulted images again into the RGB domain. Figure 4 presents the flowchart of the neutrosophic RGB conversion.

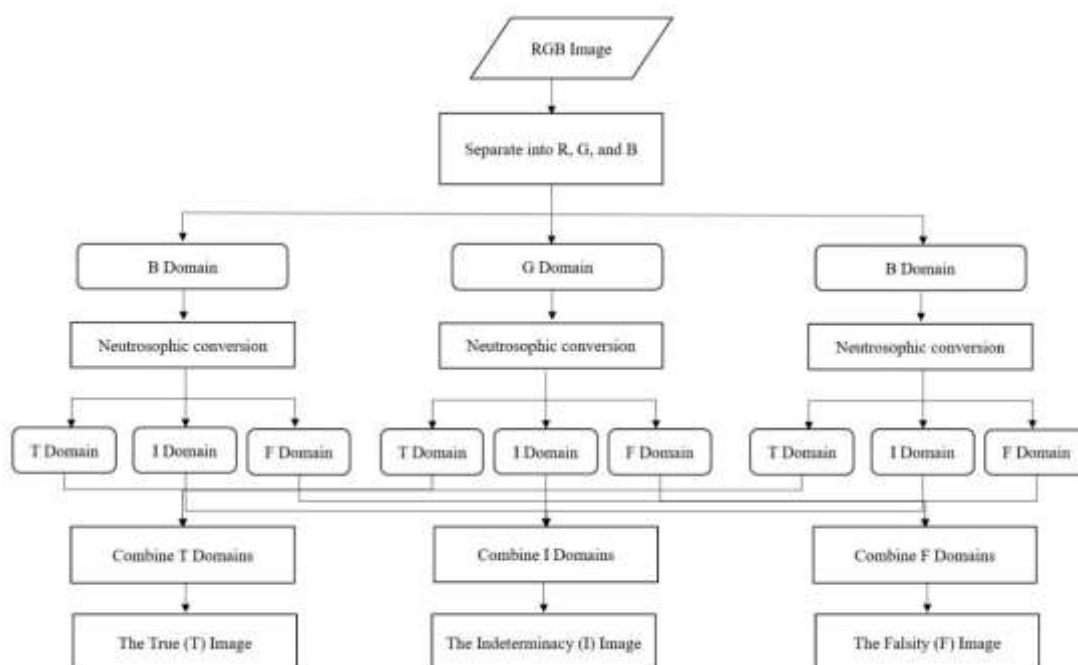
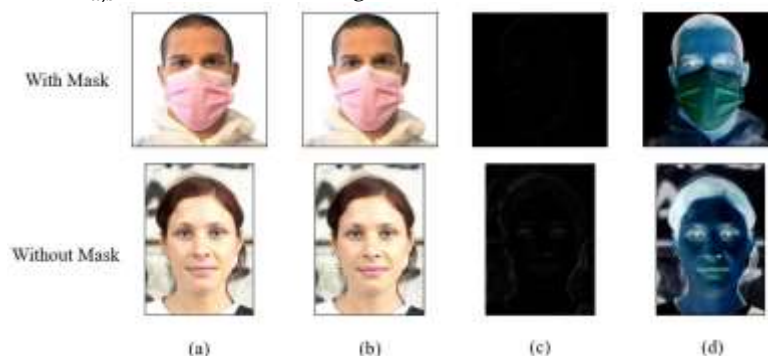


Figure 4. Neutrosophic RGB conversion flow chart

Figure 5 illustrates samples of  $(T_{a,b}, I_{a,b}, F_{a,b})$  images after performing neutrosophic image transformation in the different domains (T, I, F). Where  $T_{a,b}$  domain is masked face object,  $I_{a,b}$  domain is the edges and  $F_{a,b}$  domain is the background.



**Figure 5.** Different neutrosophic RGB pictures domains were (a) original RGB images, (b) True domain, (c) Indeterminacy, and (d) Falsity domain pictures for two classes in the dataset.

#### 4.2. AlexNet as Features Extraction

AlexNet is a deep transfer learning technique based on the convolution and pooling [42]. AlexNet is an 8-layer deep network that begins with a convolution layer and ends with a fully linked layer, as illustrated in Figure 6. To enhance our model performance in classification, the final layer in AlexNet was changed and replaced with two machine learning classifiers, SVM and DT, as shown in Figure 7. This study's primary contribution is the development of SVM and DT that do not overfit the training process.

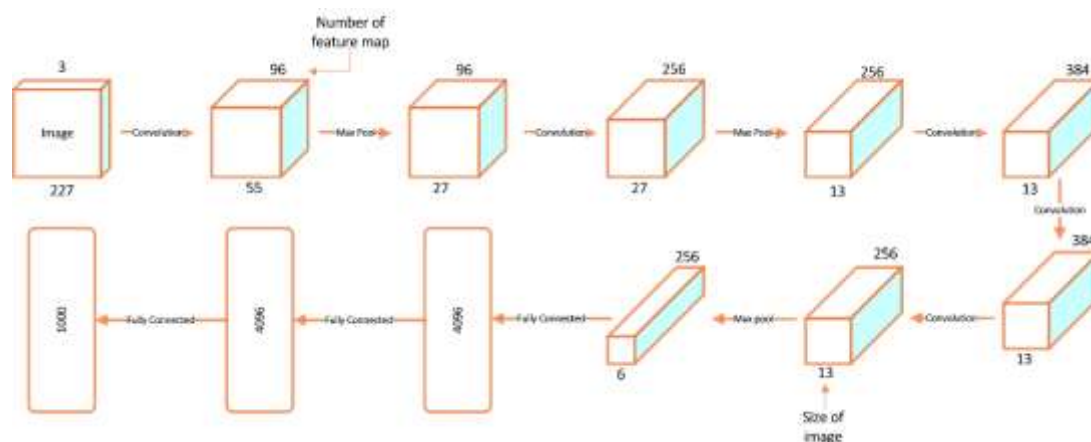


**Figure 6.** AlexNet Architecture

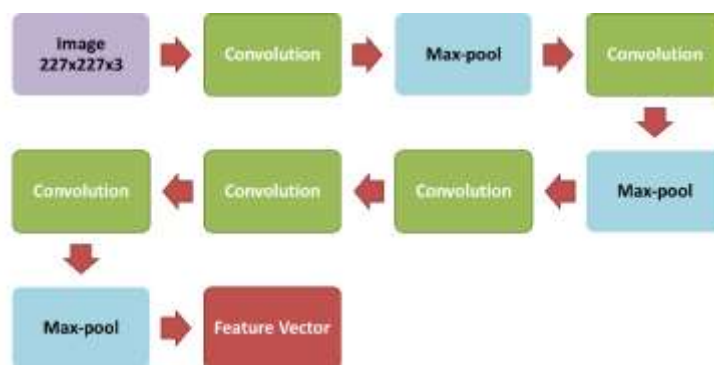


**Figure 7.** Proposed AlexNet as features extractor

### 4.3. Machine Learning Classifiers

SVM is a discriminative classifier based on hinge function  $H_v$  as illustrated in Equation 5. The output  $y$  is calculated based on  $w$  and  $d$  of linear classification as illustrated in equation 6. Where  $g$  is a class between 0 to 1. To minimize the SVM function, we implemented a loss function as shown in Equation 7 [43] , [44]. SVM maximize the distance between no mask and mask face class points as shown in Figure 8. DT is a graph of classification technique in the form of a tree model. Entropy and information gain are the main formula to calculate DT as illustrated in equation 8,9. Where  $v$  is related data, and  $u$  is a no masked face and masked face, and  $p(u_i)$  is the degree of  $u$  class. Information Gain (IG) is calculated as shown in equation 9. Where  $d$  is a subset of related data [45] , [46].

$$H_v = \max(0, 1 - g_v y) \tag{5}$$

$$y = (w \cdot x - d) \tag{6}$$

$$f = \frac{1}{u} \sum_{j=1}^u \max(0, H_j) \tag{7}$$

$$En(v) = \sum_{i=1}^c -p(u_i) \cdot \log(p(u_i)) \tag{8}$$

$$IG = En(v) - \sum_{d \in v} p(v) En(v) \tag{9}$$

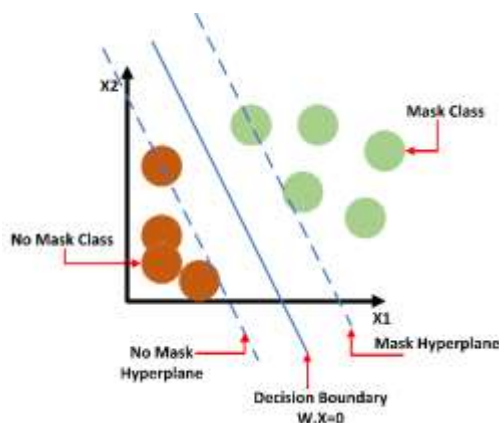


Figure 8. Illustrate how SVM work to classify masked face

## 5. Results and Discussions

All the experiments were conducted on a computer server outfitted with an Intel Xeon CPU (2 GHz) and 96 GB of RAM. The MATLAB software program was chosen for this study to create and implement the numerous experimental trails. During the experiments, the following specifications are chosen:

- Two classifiers (decision trees, and Support Vector Machine).
- Four domains of dataset images:
  - The original dataset domain (RGB).
  - The domain of the True (T) neutrosophic.
  - The domain of the Indeterminacy (I) neutrosophic.
  - The domain of the Falsity (F) neutrosophic.

- The dataset is divided into three components (70 percent of the data for the training process, 10 percent for the validation process, and 20 percent for the testing process).

Comprehensive research must examine how various classifiers perform on every dataset in order to investigate the ability of classifiers to generalize different datasets. The most common performance measures in machine learning evaluation models are, Accuracy, Precision, Recall, and F1 Score [47], and they are presented from Equation (10) to Equation (13).

$$\text{Accuracy} = \frac{\text{TPos} + \text{TNeg}}{(\text{TPos} + \text{FPos}) + (\text{TNeg} + \text{FNeg})} \quad (10)$$

$$\text{Precision} = \frac{\text{TPos}}{(\text{TPos} + \text{FPos})} \quad (11)$$

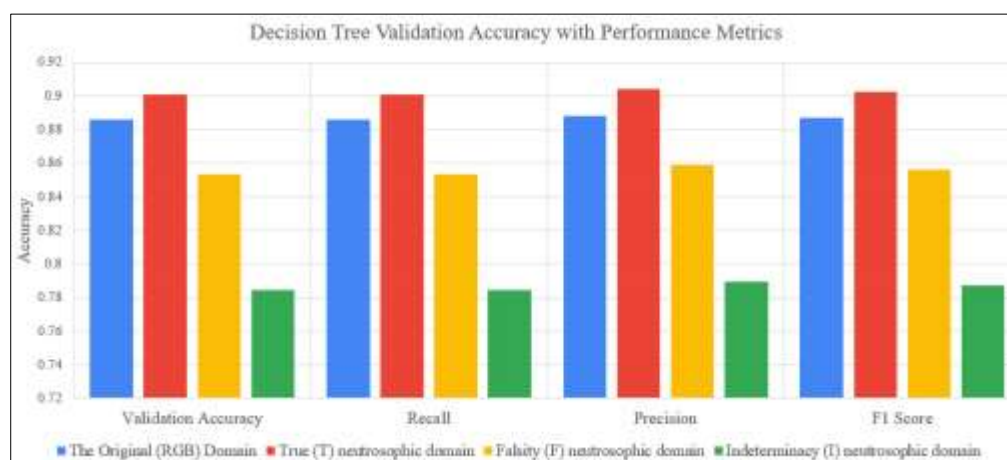
$$\text{Recall} = \frac{\text{TPos}}{(\text{TPos} + \text{FNeg})} \quad (12)$$

$$\text{F1 Score} = 2 * \frac{\text{Precision} * \text{Recall}}{(\text{Precision} + \text{Recall})} \quad (13)$$

Where TPos denotes the total number of True Positive samples, TNeg denotes the total number of True Negative samples, FPos denotes the total number of False Positive samples, and FNeg denotes the total number of False Negative samples from a confusion matrix. The findings of the experiments will be reported in three subsections. The first subsection will provide the findings acquired using a decision tree classifier, while the second subsection will give the results obtained using the SVM classifier. The third component will present a comparison outcome with similar research.

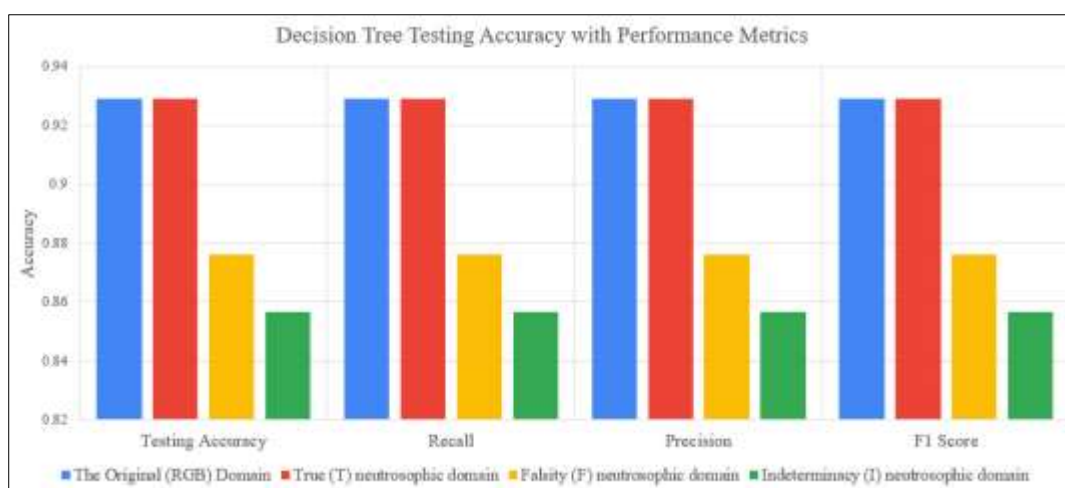
### 5.1. Experimental Results for DT Classifier

The first metric to be measured is the validation accuracy along with the other performance metrics. Validation accuracy is vital as it reflects the accuracy of the classifier during and after the training. The validation accuracy is calculated over 10% of the dataset [48]. Figure 9 depicts the validation accuracy of a decision tree classifier together with performance metrics for four domains of dataset images.



**Figure 9.** Validation accuracy and performance metrics for a DT classifier for four dataset image domains

Figure 9 illustrates that The True (T) neutrosophic domain achieved the highest possible validation accuracy with 90% while the original dataset validation accuracy is 88%. The improvement of validation accuracy is due to that the True (T) neutrosophic domain reflects the median actual pixel value depending on its neighbors' pixels. The performance metrics also support the obtained result for the achieved validation accuracy for True (T) neutrosophic domain with 0.9009, 0.9009, and 0.9039 for recall, precision, and F1 score accordingly. In Indeterminacy (I) neutrosophic domain achieved the least possible validation accuracy with performance metrics as according to the nature of the dataset, the borders of images which is the output result for the Indeterminacy (I) neutrosophic domain are not enough to improve the accuracy to differentiate between the masked and unmasked face images. Also, in the Falsity (F) neutrosophic domain, the validation accuracy is decreased than the validation accuracy for the original dataset. As in the Falsity (F) neutrosophic domain, some features are vanished due to the conversion process which reflected in the validation accuracy and other performance metrics. Validation accuracy does not reflect an accurate accuracy for the model as it is only present 10% of the dataset. So, the testing accuracy which is calculated over 20% will be more accurate and insightful for the proposed model. Figure 10 depicts the decision tree classifier's testing accuracy along with performance metrics for four domains of dataset images.



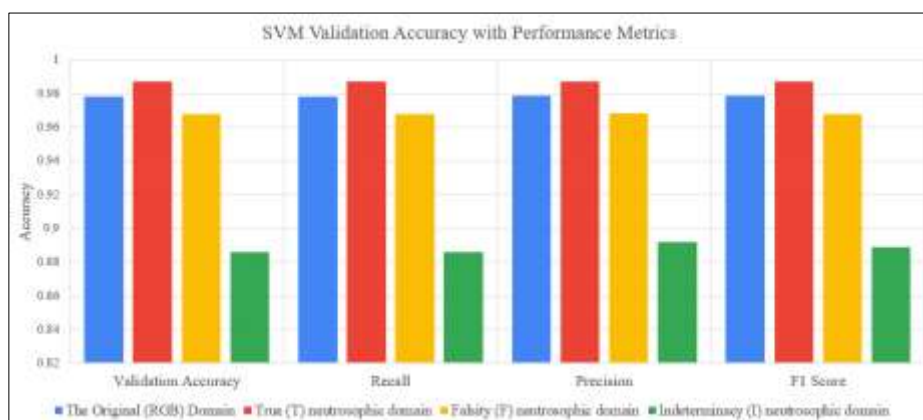
**Figure 10.** For four domains of dataset pictures, the DT classifier's accuracy was tested using performance measures.

Figure 10 illustrates that the testing accuracy with performance metrics for the original and the True (T) neutrosophic domain was the highest. The testing accuracy for both domains was 92.92%. With the same achieved performance metrics accuracy for both domains. True (T) neutrosophic domain doesn't improve the testing accuracy while the Indeterminacy (I) neutrosophic domain, and the Falsity (F) neutrosophic domain decrease the testing accuracy for the original dataset from 0.92 to 0.87 by using the Falsity (F) neutrosophic domain, and from 0.92 to 0.85 by using the Indeterminacy (I) neutrosophic domain. The reason is some of the important features in the images were disappeared due to the conversion process and the boundaries of the image for objects in the images are not enough to differentiate between the masked and the unmasked class.

To conclude this subsection concerning the decision tree classifier accuracy, the decision tree classifier was able to classify between the masked and unmasked face images using the original domain or the True (T) neutrosophic domain with a testing accuracy of 0.92 % along with performance metrics with the same value of accuracy of 0.92%.

## 5.2. Experimental Results for SVM Classifier

The validation accuracy with associated performance measures is the first statistic to be measured. Figure 11 depicts the validation accuracy of the SVM classifier together with performance characteristics for the four dataset picture domains.



**Figure 11.** Validation accuracy of the SVM classifier using performance indicators for four dataset image domains.

Figure 11 shows that for each of the four domains, the SVM classifier outperforms the decision tree classifier in terms of validation accuracy. The SVM scores 0.9784 in validation accuracy in the original RGB domain, whereas the decision tree classifier reaches 0.8858. The same behavior is repeated in all the other neutrosophic domains. The highest accuracy possible achieved by the True (T) neutrosophic domain with 0.9871 validation accuracy. The performance metrics strengthen the validation accuracy for the True (T) neutrosophic domain with the same value of validation accuracy 0.9871 for recall, precision, and F1 score. Figure 12 depicts the SVM classifier's testing accuracy as well as performance metrics for four dataset image domains.

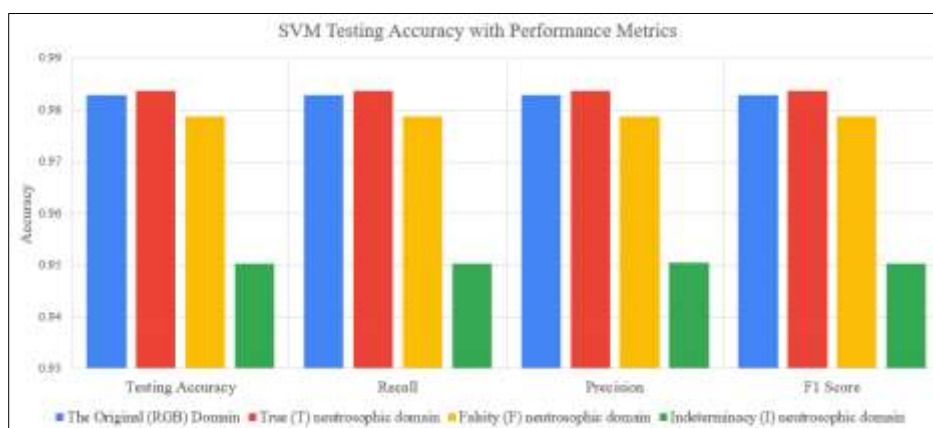


**Figure 12.** For four domains of image pictures, the SVM classifier's accuracy was tested using performance measures.

The testing accuracy is an accurate measure for the model accuracy as it presents a large sample of data (20%). Figure 12 illustrates the SVM classifier achieves higher testing accuracy than the decision tree classifier in the four domains of images. In the True (T) neutrosophic domain, the SVM classifier achieves 0.9837 in the testing accuracy while the decision tree classifier achieved 0.9292. The improvement in testing accuracy by using the SVM classifier is notable and strengthened by the calculated performance metrics over the decision tree classifier.

It is clearly shown in Figure 12 that the True (T) neutrosophic domain achieves the highest accuracy possible with 0.9837 while the nearest accuracy achieved by the original RGB with 0.9829.

The difference is not very large, but it is considered an improvement for the testing accuracy of the proposed model. This improvement in the True (T) neutrosophic domain is due to that the True (T) neutrosophic domain correctly represent the features of the image which help in classifying between masked and unmasked face images correctly.

Figure 13 depicts the time spent by the various classifiers throughout the training process. It is well understood that the spent time is proportional to the dataset size and machine capabilities, yet it provides an indication of the classifier's performance.

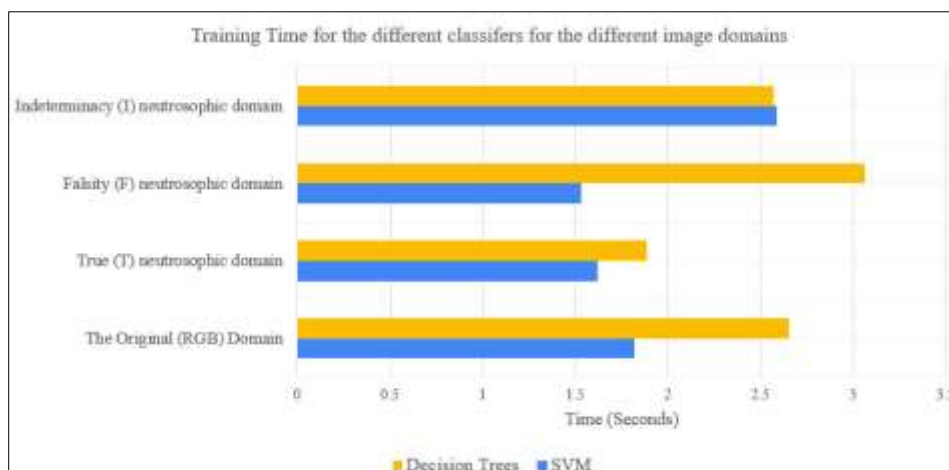


Figure 13. Training time spent by various classifiers for various image domains.

Figure 13 shows that the SVM classifier required less time to train in three of the four domains. The original domain RGB domain, the True (T) neutrosophic domain, and the Falsity (F) neutrosophic domain are the domains in which the SVM classifier obtained less time in training. To summaries this part, it is apparent that the SVM classifier outperforms the decision tree classifier in terms of validation, testing accuracy, performance metrics, and training time. With testing accuracy and performance metrics equal to 0.9837, the SVM classifier obtained the highest achievable accuracy in the True (T) neutrosophic domain.

The confusion matrix is also an excellent indicator of the performance of the model as it views more insights about the testing accuracy for every class in the dataset. Figure 14 presents the confusion matrix for the SVM classifier for the original RGB domain, and the True (T) neutrosophic domain.

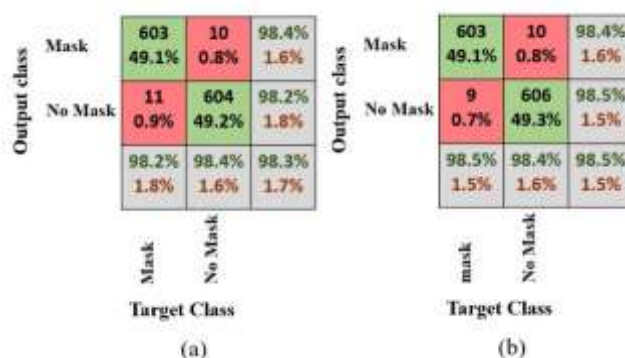


Figure 14. Confusion matrix for (a) the original RGB domain, and (b) the True (T) neutrosophic domain

Figure 14 shows that the accuracy for the face "Mask" class is 98.4 percent for both the original RGB domain and the True (T) neutrosophic domain. The improvement is in the face "No Mask" class,

where the testing accuracy is 98.5 for the True (T) neutrosophic domain and 98.2 percent for the original RGB domain.

### 5.3. Comparative Results

The study described in [37] employed the RMF dataset, and their model obtained testing accuracy ranging from 50% to 95%. The testing accuracy in the current work is 98.37% when utilizing the SVM classifier and the True (T) neutrosophic domain. According to the authors of the dataset [38], there is no documented accuracy for the simulated masked dataset SMF, there is no reported accuracy according to the author of the dataset. In this paper, we use the SVM classifier and the True (T) neutrosophic to achieve 98.37 percent testing accuracy. Table 1 compares related studies and prospective efforts that use the same datasets.

**Table 1.** A table comparing similar works and prospective efforts that use the same datasets

	<b>Short description</b>	<b>Accuracy</b>
[37]	key features extractions in visible parts of the masked face, such as face contour, ocular and periocular details, forehead with nearest neighbor algorithm.	50% to 95%
Proposed model	SVM classifier with the True (T) neutrosophic	98.37%

## 6. Conclusion and Future Works

A worldwide health catastrophe is triggered by the COVID-19 coronavirus pandemic. Governments all around the globe are battling to halt the spread of this sort of virus. Protection against COVID-19 infection, according to the World Health Organization (WHO), is a required countermeasure. Wearing a face mask in public places is one of the required countermeasures. A face mask classification model based on neutrosophic RGB with Convolutional Neural Network (CNN) for feature extraction and conventional machine learning was presented in this study. The suggested model was divided into three stages, the first of which was the conversion to the neutrosophic RGB domain. This study was regarded one of the earliest trails of using neutrosophic RGB conversion, since it was frequently utilized in grayscale picture conversion. The second state was the features extraction using Alexnet. It will be used as a feature extractor throughout the proposed model. The third phase was the detection model using classical machine learning. Two classical machine learning algorithms were investigated, and they were the decision tress classifier and Support Vector Machine (SVM). A dataset consisted of two different datasets, and they were the Real-World Mask Face dataset (RMF) and the Simulated Masked Face dataset (SMF). The combined dataset contained two classes (with a mask, and without a mask). The SVM classifier using the True (T) neutrosophic domain had the highest testing accuracy with 98.37 percent, according to the experimental findings. The acquired findings were validated by performance measures like as Precision, Recall, and F1 Score. At the end of the study, a comparison result was obtained, and the suggested model outperformed the findings of the related works in terms of testing accuracy. Deeper deep learning models for feature extraction, such as Resnet50 or Inception-ResNet-v2, may be included as one of the potential future efforts. In addition, other traditional machine learning techniques, such as Ensemble classifier, may be used to improve testing accuracy.

## References

- [1] "WHO Coronavirus (COVID-19) Dashboard." <https://covid19.who.int> (accessed Dec. 24, 2021).
- [2] M. Loey, F. Smarandache, and N. E. M. Khalifa, "Within the Lack of Chest COVID-19 X-ray Dataset: A Novel Detection Model Based on GAN and Deep Transfer Learning," *Symmetry*, vol. 12, no. 4, Art. no. 4, Apr. 2020, doi: 10.3390/sym12040651.
- [3] Y. Goh, B. Y. Q. Tan, C. Bhartendu, J. J. Y. Ong, and V. K. Sharma, "The face mask: How a real protection becomes a psychological symbol during Covid-19?," *Brain. Behav. Immun.*, vol. 88, pp. 1–5, Aug. 2020, doi: 10.1016/j.bbi.2020.05.060.
- [4] R. O. J. H. Stutt, R. Retkute, M. Bradley, C. A. Gilligan, and J. Colvin, "A modelling framework to assess the likely effectiveness of facemasks in combination with 'lock-down' in managing the COVID-19 pandemic," *Proc. R. Soc. Math. Phys. Eng. Sci.*, vol. 476, no. 2238, p. 20200376, Jun. 2020, doi: 10.1098/rspa.2020.0376.
- [5] S. Feng, C. Shen, N. Xia, W. Song, M. Fan, and B. J. Cowling, "Rational use of face masks in the COVID-19 pandemic," *Lancet Respir. Med.*, vol. 8, no. 5, pp. 434–436, May 2020, doi: 10.1016/S2213-2600(20)30134-X.
- [6] D. M. Altmann, D. C. Douek, and R. J. Boyton, "What policy makers need to know about COVID-19 protective immunity," *The Lancet*, vol. 395, no. 10236, pp. 1527–1529, May 2020, doi: 10.1016/S0140-6736(20)30985-5.
- [7] B. Javid, "Across the world, face masks are becoming mandatory. Why not in the UK?," *The Guardian*, Apr. 24, 2020. Accessed: Dec. 24, 2021. [Online]. Available: <https://www.theguardian.com/commentisfree/2020/apr/24/face-masks-mandatory-spread-coronavirus-government>
- [8] M. Loey, M. Naman, and H. Zayed, "Deep Transfer Learning in Diagnosing Leukemia in Blood Cells," *Computers*, vol. 9, no. 2, Art. no. 2, Jun. 2020, doi: 10.3390/computers9020029.
- [9] R. Vaishya, M. Javaid, I. H. Khan, and A. Haleem, "Artificial Intelligence (AI) applications for COVID-19 pandemic," *Diabetes Metab. Syndr. Clin. Res. Rev.*, vol. 14, no. 4, pp. 337–339, Jul. 2020, doi: 10.1016/j.dsx.2020.04.012.
- [10] M. Loey, G. Manogaran, M. H. N. Taha, and N. E. M. Khalifa, "Fighting against COVID-19: A novel deep learning model based on YOLO-v2 with ResNet-50 for medical face mask detection," *Sustain. Cities Soc.*, vol. 65, p. 102600, Feb. 2021, doi: 10.1016/j.scs.2020.102600.
- [11] P. Nagrath, R. Jain, A. Madan, R. Arora, P. Kataria, and J. Hemanth, "SSDMNV2: A real time DNN-based face mask detection system using single shot multibox detector and MobileNetV2," *Sustain. Cities Soc.*, vol. 66, p. 102692, Mar. 2021, doi: 10.1016/j.scs.2020.102692.
- [12] K. Ahmed, S. Abdelghafar, A. Salama, N. E. M. Khalifa, A. Darwish, and A. E. Hassanien, "Tracking of COVID-19 Geographical Infections on Real-Time Tweets." 2021.
- [13] A. El-Aziz, A. Atrab, N. E. M. Khalifa, A. Darwsih, and A. E. Hassanien, "The role of emerging technologies for combating COVID-19 pandemic," in *Digital Transformation and Emerging Technologies for Fighting COVID-19 Pandemic: Innovative Approaches*, Springer, 2021, pp. 21–41.
- [14] A. A. Abd El-Aziz, N. E. M. Khalifa, and A. E. Hassanien, "Exploring the Impacts of COVID-19 on Oil and Electricity Industry," in *The Global Environmental Effects During and Beyond COVID-19*, Springer, 2021, pp. 149–161.
- [15] N. E. KHALIFA, G. MANOGARAN, M. H. N. TAHA, and M. LOEY, "The classification of possible Coronavirus treatments on a single human cell using deep learning and machine learning approaches," *J. Theor. Appl. Inf. Technol.*, vol. 99, no. 21, 2021.

- [16] J. Civit-Masot, F. Luna-Perejón, M. Domínguez Morales, and A. Civit, "Deep Learning System for COVID-19 Diagnosis Aid Using X-ray Pulmonary Images," *Appl. Sci.*, vol. 10, no. 13, Art. no. 13, Jan. 2020, doi: 10.3390/app10134640.
- [17] A. Waheed, M. Goyal, D. Gupta, A. Khanna, F. Al-Turjman, and P. R. Pinheiro, "CovidGAN: Data Augmentation Using Auxiliary Classifier GAN for Improved Covid-19 Detection," *IEEE Access*, vol. 8, pp. 91916–91923, 2020, doi: 10.1109/ACCESS.2020.2994762.
- [18] N. Narayan Das, N. Kumar, M. Kaur, V. Kumar, and D. Singh, "Automated Deep Transfer Learning-Based Approach for Detection of COVID-19 Infection in Chest X-rays," *IRBM*, Jul. 2020, doi: 10.1016/j.irbm.2020.07.001.
- [19] A. A. Ardakani, A. R. Kanafi, U. R. Acharya, N. Khadem, and A. Mohammadi, "Application of deep learning technique to manage COVID-19 in routine clinical practice using CT images: Results of 10 convolutional neural networks," *Comput. Biol. Med.*, vol. 121, p. 103795, Jun. 2020, doi: 10.1016/j.combiomed.2020.103795.
- [20] F. Smarandache, "Neutrosophic Logic and Set." 1995.
- [21] F. Smarandache, "A unifying field in logics. neutrosophy: Neutrosophic probability, set and logic." American Research Press, Rehoboth, 1999.
- [22] M. Ali, I. Deli, and F. Smarandache, "The theory of neutrosophic cubic sets and their applications in pattern recognition," *J. Intell. Fuzzy Syst.*, vol. 30, no. 4, pp. 1957–1963, Jan. 2016, doi: 10.3233/IFS-151906.
- [23] A. Salama, "Basic Structure of Some Classes of Neutrosophic Crisp Nearly Open Sets & Possible Application to GIS Topology," *Neutrosophic Sets Syst.*, vol. 7, no. 1, Jan. 2015, [Online]. Available: [https://digitalrepository.unm.edu/nss\\_journal/vol7/iss1/4](https://digitalrepository.unm.edu/nss_journal/vol7/iss1/4)
- [24] V. Christianto and F. Smarandache, "A Review of Seven Applications of Neutrosophic Logic: In Cultural Psychology, Economics Theorizing, Conflict Resolution, Philosophy of Science, etc.," *J*, vol. 2, no. 2, Art. no. 2, Jun. 2019, doi: 10.3390/j2020010.
- [25] A. M. Anter and A. E. Hassenian, "CT liver tumor segmentation hybrid approach using neutrosophic sets, fast fuzzy c-means and adaptive watershed algorithm," *Artif. Intell. Med.*, vol. 97, pp. 105–117, Jun. 2019, doi: 10.1016/j.artmed.2018.11.007.
- [26] R. Bausys, G. Kazakeviciute-Januskeviciene, F. Cavallaro, and A. Usovaite, "Algorithm Selection for Edge Detection in Satellite Images by Neutrosophic WASPAS Method," *Sustainability*, vol. 12, no. 2, Art. no. 2, Jan. 2020, doi: 10.3390/su12020548.
- [27] F. Smarandache *et al.*, "1 - Introduction to neutrosophy and neutrosophic environment," in *Neutrosophic Set in Medical Image Analysis*, Y. Guo and A. S. Ashour, Eds. Academic Press, 2019, pp. 3–29. doi: 10.1016/B978-0-12-818148-5.00001-1.
- [28] "Neutrosophic Sets - an overview | ScienceDirect Topics." <https://www.sciencedirect.com/topics/computer-science/neutrosophic-sets> (accessed Dec. 24, 2021).
- [29] M. Jayaraman, K. Vellingiri, and Y. Guo, "4 - Neutrosophic set in medical image denoising," in *Neutrosophic Set in Medical Image Analysis*, Y. Guo and A. S. Ashour, Eds. Academic Press, 2019, pp. 77–100. doi: 10.1016/B978-0-12-818148-5.00004-7.
- [30] "Sensors | Free Full-Text | Identifying Facemask-Wearing Condition Using Image Super-Resolution with Classification Network to Prevent COVID-19." <https://www.mdpi.com/1424-8220/20/18/5236> (accessed Dec. 24, 2021).

- [31] "Facial emotion recognition using convolutional neural networks (FERC) | SpringerLink." <https://link.springer.com/article/10.1007/s42452-020-2234-1> (accessed Dec. 24, 2021).
- [32] N. Ud Din, K. Javed, S. Bae, and J. Yi, "A Novel GAN-Based Network for Unmasking of Masked Face," *IEEE Access*, vol. 8, pp. 44276–44287, 2020, doi: 10.1109/ACCESS.2020.2977386.
- [33] C. Li, R. Wang, J. Li, and L. Fei, "Face Detection Based on YOLOv3," in *Recent Trends in Intelligent Computing, Communication and Devices*, Singapore, 2020, pp. 277–284. doi: 10.1007/978-981-13-9406-5\_34.
- [34] V. Jain and E. Learned-miller, "FDDB: A benchmark for face detection in unconstrained settings," 2010.
- [35] C. Su, Y. Yan, S. Chen, and H. Wang, "An efficient deep neural networks training framework for robust face recognition," in *2017 IEEE International Conference on Image Processing (ICIP)*, Sep. 2017, pp. 3800–3804. doi: 10.1109/ICIP.2017.8296993.
- [36] E. Learned-Miller, G. B. Huang, A. RoyChowdhury, H. Li, and G. Hua, "Labeled Faces in the Wild: A Survey," in *Advances in Face Detection and Facial Image Analysis*, M. Kawulok, M. E. Celebi, and B. Smolka, Eds. Cham: Springer International Publishing, 2016, pp. 189–248. doi: 10.1007/978-3-319-25958-1\_8.
- [37] Z. Wang *et al.*, "Masked Face Recognition Dataset and Application," *ArXiv200309093 Cs*, Mar. 2020, Accessed: Dec. 24, 2021. [Online]. Available: <http://arxiv.org/abs/2003.09093>
- [38] P. Bhandary, *prajnasb/observations*. 2021. Accessed: Dec. 24, 2021. [Online]. Available: <https://github.com/prajnasb/observations>
- [39] I. Deli, M. Ali, and F. Smarandache, "Bipolar neutrosophic sets and their application based on multi-criteria decision making problems," in *2015 International Conference on Advanced Mechatronic Systems (ICAMechS)*, Aug. 2015, pp. 249–254. doi: 10.1109/ICAMechS.2015.7287068.
- [40] F. Smarandache and L. Vlădăreanu, "Applications of neutrosophic logic to robotics: An introduction," in *2011 IEEE International Conference on Granular Computing*, Nov. 2011, pp. 607–612. doi: 10.1109/GRC.2011.6122666.
- [41] F. Özyurt, E. Sert, E. Avci, and E. Dogantekin, "Brain tumor detection based on Convolutional Neural Network with neutrosophic expert maximum fuzzy sure entropy," *Measurement*, vol. 147, p. 106830, Dec. 2019, doi: 10.1016/j.measurement.2019.07.058.
- [42] A. Krizhevsky, I. Sutskever, and G. E. Hinton, "Imagenet classification with deep convolutional neural networks," in *Advances in Neural Information Processing Systems*, p. 2012.
- [43] A. Çayir, I. Yenidoğan, and H. Dağ, "Feature Extraction Based on Deep Learning for Some Traditional Machine Learning Methods," in *2018 3rd International Conference on Computer Science and Engineering (UBMK)*, Sep. 2018, pp. 494–497. doi: 10.1109/UBMK.2018.8566383.
- [44] M. Jogin, Mohana, M. S. Madhulika, G. D. Divya, R. K. Meghana, and S. Apoorva, "Feature Extraction using Convolution Neural Networks (CNN) and Deep Learning," in *2018 3rd IEEE International Conference on Recent Trends in Electronics, Information Communication Technology (RTEICT)*, May 2018, pp. 2319–2323. doi: 10.1109/RTEICT42901.2018.9012507.
- [45] "Overview of use of decision tree algorithms in machine learning | IEEE Conference Publication | IEEE Xplore." <https://ieeexplore.ieee.org/document/5991826> (accessed Dec. 24, 2021).
- [46] P.-L. Tu and J.-Y. Chung, "A new decision-tree classification algorithm for machine learning," in *Proceedings Fourth International Conference on Tools with Artificial Intelligence TAI '92*, Nov. 1992, pp. 370–377. doi: 10.1109/TAI.1992.246431.

- [47] C. Goutte and E. Gaussier, "A Probabilistic Interpretation of Precision, Recall and F-Score, with Implication for Evaluation," in *Advances in Information Retrieval*, Berlin, Heidelberg, 2005, pp. 345–359. doi: 10.1007/978-3-540-31865-1\_25.
- [48] M. Loey, G. Manogaran, M. H. N. Taha, and N. E. M. Khalifa, "A hybrid deep transfer learning model with machine learning methods for face mask detection in the era of the COVID-19 pandemic," *Measurement*, vol. 167, p. 108288, Jan. 2021, doi: 10.1016/j.measurement.2020.108288.

Received: Feb 8, 2022. Accepted: Jun 2, 2022